

Article

# Subgenome Discrimination in *Brassica* and *Raphanus* Allopolyploids Using Microsatellites

Nicole Bon Campomayor<sup>1,†</sup>, Nomar Espinosa Waminal<sup>1,†</sup> , Byung Yong Kang<sup>1</sup>, Thi Hong Nguyen<sup>1</sup>, Soo-Seong Lee<sup>2</sup>, Jin Hoe Huh<sup>3</sup> and Hyun Hee Kim<sup>1,\*</sup>

<sup>1</sup> Department of Chemistry and Life Science, BioScience Institute, Sahmyook University, Seoul 01795, Korea; nbacampomayor@syuin.ac.kr (N.B.C.); newaminal@syu.ac.kr (N.E.W.); kang1969@syu.ac.kr (B.Y.K.); nguyenhong@syuin.ac.kr (T.H.N.)

<sup>2</sup> BioBreeding Institute, Ansung 17544, Korea; sslee0872@hotmail.com

<sup>3</sup> Department of Agriculture, Forestry and Bioresources, Plant Genomics and Breeding Institute, Seoul National University, Seoul 08826, Korea; huhjh@snu.ac.kr

\* Correspondence: kimhh@syu.ac.kr; Tel.: +82-2-3399-1715

† These authors contributed equally to this work.



**Citation:** Campomayor, N.B.; Waminal, N.E.; Kang, B.Y.; Nguyen, T.H.; Lee, S.-S.; Huh, J.H.; Kim, H.H. Subgenome Discrimination in *Brassica* and *Raphanus* Allopolyploids Using Microsatellites. *Cells* **2021**, *10*, 2358. <https://doi.org/10.3390/cells10092358>

Academic Editor: Laurens Pauwels

Received: 27 July 2021

Accepted: 3 September 2021

Published: 8 September 2021

**Publisher's Note:** MDPI stays neutral with regard to jurisdictional claims in published maps and institutional affiliations.



**Copyright:** © 2021 by the authors. Licensee MDPI, Basel, Switzerland. This article is an open access article distributed under the terms and conditions of the Creative Commons Attribution (CC BY) license (<https://creativecommons.org/licenses/by/4.0/>).

**Abstract:** Intergeneric crosses between *Brassica* species and *Raphanus sativus* have produced crops with prominent shoot and root systems of *Brassica* and *R. sativus*, respectively. It is necessary to discriminate donor genomes when studying cytogenetic stability in distant crosses to identify homologous chromosome pairing, and microsatellite repeats have been used to discriminate subgenomes in allopolyploids. To identify genome-specific microsatellites, we explored the microsatellite content in three *Brassica* species (*B. rapa*, AA, *B. oleracea*, CC, and *B. nigra*, BB) and *R. sativus* (RR) genomes, and validated their genome specificity by fluorescence in situ hybridization. We identified three microsatellites showing A, C, and B/R genome specificity. ACBR\_msat14 and ACBR\_msat20 were detected in the A and C chromosomes, respectively, and ACBR\_msat01 was detected in B and R genomes. However, we did not find a microsatellite that discriminated the B and R genomes. The localization of ACBR\_msat20 in the 45S rDNA array in  $\times$ *Brassicoraphanus* 977 corroborated the association of the 45S rDNA array with genome rearrangement. Along with the rDNA and telomeric repeat probes, these microsatellites enabled the easy identification of homologous chromosomes. These data demonstrate the utility of microsatellites as probes in identifying subgenomes within closely related *Brassica* and *Raphanus* species for the analysis of genetic stability of new synthetic polyploids of these genomes.

**Keywords:** allopolyploid; *Brassica*; fluorescence in situ hybridization; karyotype; microsatellite; *Raphanus*

## 1. Introduction

The genus *Brassica* (Brassicaceae) includes several economically valuable crops that are used as oilseeds, condiments, culinary vegetables [1,2], and sources of health-promoting phytochemicals [3,4]. *Brassica* is also a good model for studying polyploidization because of numerous intercrossing and morphological variants [5,6]. The genetic relationship of the six most economically important *Brassica* species was described in U's triangle [7]. These include three diploids, *B. rapa* (AA genome,  $2n = 2x = 20$ ), *B. nigra* (BB,  $2n = 2x = 16$ ), and *B. oleracea* (CC,  $2n = 2x = 18$ ), and their allotetraploid hybrids, *B. juncea* (AABB,  $2n = 4x = 36$ ), *B. napus* (AACC,  $2n = 4x = 38$ ), and *B. carinata* (BBCC,  $2n = 4x = 34$ ).

Like many *Brassica* species, *R. sativus* L. (RR,  $2n = 2x = 18$ ) has also been cultivated worldwide [8,9]. *R. sativus* is valued more for its roots than *Brassica* species, whose shoots are the primary commodities. Breeders have attempted to synthesize hybrids with shoot and root features of *Brassica* crops and *R. sativus*, respectively, to maximize the use of plant parts for culinary purposes [10]. Therefore, several synthetic crops that involved crosses between the A, C, B, and R genomes have been generated [11–15]. One such example is the

intergeneric allotetraploid  $\times Brassicoraphanus$ , commonly known as 'Baemoochae', which resulted from a cross between *B. rapa* ssp. *pekinensis* L. and *R. sativus* L. [10,16].

However, due to frequent genetic instability of the selected phenotypes, only a few stable  $\times Brassicoraphanus$  lines have been successfully registered as commercial cultivars to date. One of these is "BB#1" ( $2n = 38$ , AARR genome), which was stabilized through induced microspore mutation of the intergeneric hybrid between *B. rapa* cv. Weongyo#207 and *R. sativus* cv. Baekgyoung [10,17,18].

Several lines involving multiple genomes have also been developed from crosses of synthetic allotetraploids. One example is hybrid  $\times Brassicoraphanus$  977 (Supplementary Figure S1), which possibly carries chromosome blocks from the A, C, and R genomes, considering its genomic background from a cross between two  $\times Brassicoraphanus$  allotetraploids, BB#50 (AARR,  $2n = 4x = 38$ ) and "Mooyangchae" (RRCC,  $2n = 4x = 36$ ), a fertile amphidiploid progeny between *Raphanus sativus* cv. HQ-04 ( $2n = 2x = 18$ , RR) and *Brassica alboglabra* Bailey ( $2n = 2x = 18$ , CC) [19]. At present, the karyotype and genome composition of  $\times Brassicoraphanus$  977 have not yet been reported.

It is important to identify the donor genomes of all chromosomes in  $\times Brassicoraphanus$  977 for efficient karyotyping. Genomic in situ hybridization (GISH) is a conventional technique used to analyze donor genomes in allopolyploids [20,21]. However, GISH is laborious and inefficient in discriminating the A and C *Brassica* genomes in *B. napus* [22–24]. However, GISH-like results have been achieved using conventional fluorescence in situ hybridization (FISH) with microsatellite repeats as probes instead of genomic DNA. This approach discriminated C from the A genome in *B. napus* [24,25] and the B genome in *Triticum aestivum* [26].

Microsatellites are often used in PCR-based genetic diversity studies because of their high rate of transferability to other closely and even distantly related taxa [27]. They have been used to identify subgenome alleles in some bryophytes [28]. Moreover, microsatellites are good cytogenomic markers because they are expected to be distributed evenly along chromosomes [29]. However, they have not yet been used to visually discriminate subgenomes in allopolyploid species, and there has not been an extensive comparative whole-genome microsatellite quantification and FISH analysis between the *Brassica* A, C, B, and *R. sativus* R genomes. Hence, we are advancing the use of microsatellites in analyzing their presence and absence in component chromosomes of subgenomes to identify homologous chromosomes in allopolyploids.

This study aimed to determine whether similar microsatellites, such as the C-genome-specific ones found in *B. napus*, are also found in the A, B, and R genomes. We quantified microsatellite repeats in the A, C, B, and R genomes and performed comparative FISH to identify potential genome-specific microsatellites that can be used as a cytogenomic resource in karyotyping polyploid hybrids between these four genomes. Finding similar microsatellites unique to the A, C, B, and R genomes would ease chromosome discrimination in  $\times Brassicoraphanus$  977 and other natural and synthetic allopolyploids carrying these genomes.

## 2. Materials and Methods

### 2.1. Microsatellite Mining

To analyze genome-specific microsatellites, we downloaded 100-bp whole-genome sequence reads of the four diploid A, C, B, and R genomes from NCBI (Table 1). High-quality reads representing  $0.04\text{--}0.06\times$  of the A, C, B, and R genomes [30–33] were selected using the FastQC tool in the RepeatExplorer version 2 pipeline [34]. Following a script provided in RepeatExplorer2, a long single contig was generated by concatenating all reads from each species and inserting 50-bp Ns between reads.

Each contig from the A, C, B, and R genomes was scanned for tandem repeats of  $\leq 20$  bp using Tandem Repeats Finder version 4.09 [35], and the output was sorted and quantified using the TRAP program v1 [36]. The repeat units of each microsatellite were concatenated to approximately 200 bp. To filter out redundant sequences, we grouped

similar sequences and generated consensus sequences using the *Assembly Sequence* features in the CLC Main Workbench (CLC Inc., Aarhus, Denmark). The microsatellites were named ACBR\_msat# according to the closer relationship of the A/C and B/R genomes [37], msat for “microsatellite” and the number order according to decreasing cumulative abundance. For FISH validation, we selected microsatellites with > 6 kb cumulative total bases from the A, C, B, and R genomes. A summary of the mining and FISH validation workflow is presented in Supplementary Figure S2.

**Table 1.** Description of *Brassica* and *Raphanus* next-generation sequencing reads used to generate the microsatellites and summary of the coverage.

| Species            | Cultivar               | Genome | Genome Size (Mbp) | Accession Number | Reads   | Coverage (×) |
|--------------------|------------------------|--------|-------------------|------------------|---------|--------------|
| <i>B. rapa</i>     | Chiifu-401-42          | AA     | 353               | GCA_000309985.3  | 199,662 | 0.06         |
| <i>B. oleracea</i> | TO1000                 | CC     | 522               | GCA_000695525.1  | 200,880 | 0.04         |
| <i>B. nigra</i>    | inbred line<br>YZ12151 | BB     | 468               | GCA_001682895.1  | 201,798 | 0.04         |
| <i>R. sativus</i>  | XYB36-2                | RR     | 414               | GCA_002197605.1  | 201,210 | 0.05         |

## 2.2. Designing Microsatellite Pre-Labeled Oligoprobes

We developed pre-labeled oligonucleotide probes (PLOPs) for FISH validation of candidate microsatellites (Supplementary Table S1). PLOPs were designed using the CLC Main Workbench (CLC, Inc.) and synthesized by Bio Basic Canada Inc. (Toronto, ON, Canada). In addition, we also used 5S rDNA, 45S rDNA, and telomeric repeat PLOPs for chromosome identification. The rDNA and telomeric PLOPs were designed and prepared following methods described in [38] and were purchased from Bioneer (Daejeon, Korea).

## 2.3. Plant Samples

Seeds of the four diploid and five allopolyploid species were purchased commercially and provided by the National Plant Germplasm System of the US Department of Agriculture, the National Academy of Agricultural Science of Korea, or the BioBreeding Institute, Ansong, Korea (Table 2). Seeds were germinated on filter paper and incubated at 25 °C. Harvested root tips were treated with 2 mM 8-hydroxyquinoline for 5 h at 18 °C, fixed with aceto-ethanol (1:3 v/v), and stored in 70% ethanol at 4 °C until use.

**Table 2.** List of plant materials with their corresponding haploid chromosome number, genome type, seed source, and accession number.

| Species                          | 2n | Genome Type | Source   | Accession Number |
|----------------------------------|----|-------------|--|------------------|
| <i>B. rapa</i>                   | 20 | AA          | NAAS <sup>a</sup>                              | IT 032730        |
| <i>B. oleracea</i>               | 18 | CC          | NPGS <sup>b</sup>                              | PI 24501510GI    |
| <i>B. nigra</i>                  | 16 | BB          | NPGS   | PI 649154        |
| <i>R. sativus</i>                | 18 | RR          | danong.co.kr<br>(accessed on 31<br>April 2019) | N/A              |
| <i>B. napus</i>                  | 38 | AACC        | NPGS   | TI 031006        |
| <i>B. juncea</i>                 | 36 | AABB        | NPGS   | PI 633077        |
| <i>B. carinata</i>               | 34 | BBCC        | NPGS   | Ames 2779        |
| × <i>Brassicoraphanus</i> ‘BB#1’ | 38 | AARR        | BioBreeding<br>Institute<br>(Ansong, Korea)    | PRJNA353741      |
| × <i>Brassicoraphanus</i> 977    | 38 | ARRC        | BioBreeding<br>Institute                       | N/A              |

<sup>a</sup> National Academy of Agricultural Sciences, (Jeollabuk-do, Korea); <sup>b</sup> National Plant Germplasm System, (US Department of Agriculture, USA).

#### 2.4. Chromosome Preparation

Somatic chromosome spreads were prepared following the technique described by Waminal and Kim [39]. Five meristematic tips (~2 mm) were digested with pectolytic enzyme solution (2% Cellulase R-10 (C224, Phytotechnology Laboratories, Lenexa, KS, USA) and 1% Pectolyase Y-23 (P8004.0001, Duchefa, Haarlem, The Netherlands) in 100 mM citrate buffer) at 37 °C for 90 min. Roots were transferred into a microtube with chilled Carnoy's solution and vortexed for 30 s at room temperature. The supernatant was discarded, and the pellet was resuspended in an appropriate amount of aceto-ethanol (9:1 *v/v*). The cellular suspension was pipetted onto pre-cleaned slides and pre-warmed in a humid chamber. After air-drying, slides were fixed in 2% formaldehyde [39] for 5 min, quickly rinsed with distilled water, and dehydrated in a series of ethanol treatments (70%, 90%, and 100%).

#### 2.5. FISH and Karyotyping

FISH was performed according to the modified procedure of Waminal et al. [40] and Lim et al. [41]. The FISH hybridization mixture was prepared with 100% formamide, 50% dextran sulfate, 20× SSC, 50 ng/μL of each DNA probe, and deionized water (Sigma-Aldrich, St. Louis, MO, USA). The mixture was pipetted onto each slide. Slides were incubated at 80 °C for 5 min and transferred to a humid chamber at 37 °C overnight. After overnight hybridization, incubated slides were washed in 2× SSC at room temperature (RT) for 10 min, 0.1× SSC at 42 °C for 25 min, and 2× SSC at RT for 5 min, and dehydrated in a series of alcohol (70%, 90%, 95%). Slides were air-dried and counterstained with 4',6-diaminidino-2-phenylindole (DAPI) at a ratio of 1:100 DAPI (100 μg/mL stock) and Vectashield (Vector Laboratories, Burlingame, CA, USA). Five to 10 well-spread metaphase chromosomes were chosen and were observed under an Olympus BX53 fluorescence microscope with a built-in CCD camera (CoolSNAP™ cf), using an oil lens (×100 magnification). One metaphase chromosome spread was selected as a representative for each genome for karyotype analyse. Karyograms were finalized using Adobe Photoshop CC version 25.3, whereas ideograms were generated using Adobe Illustrator CC version 22.4. Homologous chromosomes were identified based on their FISH signals, morphological characteristics, and lengths, considering previous karyotype data for *B. rapa*, *B. oleracea*, and *B. napus* [5], *B. nigra* and *B. juncea* [42], and *R. sativus* and *×Brassicoraphanus* [43].

### 3. Results

#### 3.1. Identification of Major Microsatellites in the A, C, B, and R Genomes

To capture microsatellites with higher-order organization, we loosen our definition of microsatellites from a stricter 2–5 bp [44] to an extended target length of ≤ 20 bp (Supplementary Figure S2). This configuration generated 467 microsatellites in both strand orientations, including redundant or imperfect motif sequences [45] as demonstrated by sequence clustering (Figure 1A). Among the 467 microsatellites, the A, C, and B genomes had 123 sequences each. However, the R genome had only 98. The total base count for all microsatellites in each genome represented up to 0.2–0.3% of each genome (Figure 1B). Clustering of the related sequences generated 184 unique consensus sequences. Most of these microsatellites were di- and trinucleotides (Figure 1C). Many of these sequences represented <6 kb of cumulative total bases from the A, C, B, and R genomes. We only selected microsatellites with >6 kb cumulative total bases for FISH validation because microsatellites with lower total bases may not generate detectable FISH signals. This filtering retained 22 microsatellites, of which ACBR\_msat01 had the highest cumulative total bases of ~328 kb (Figure 1D), which was distributed proportionately among the four genomes (Figure 1E and Table 3). Moreover, the ranks of the 22 microsatellites varied in each genome. For example, although the ACBR\_msat06 was ranked sixth based on cumulative abundance, it ranked third, ninth, ninth, and fourteenth in the C, A, R, and B genomes, respectively.

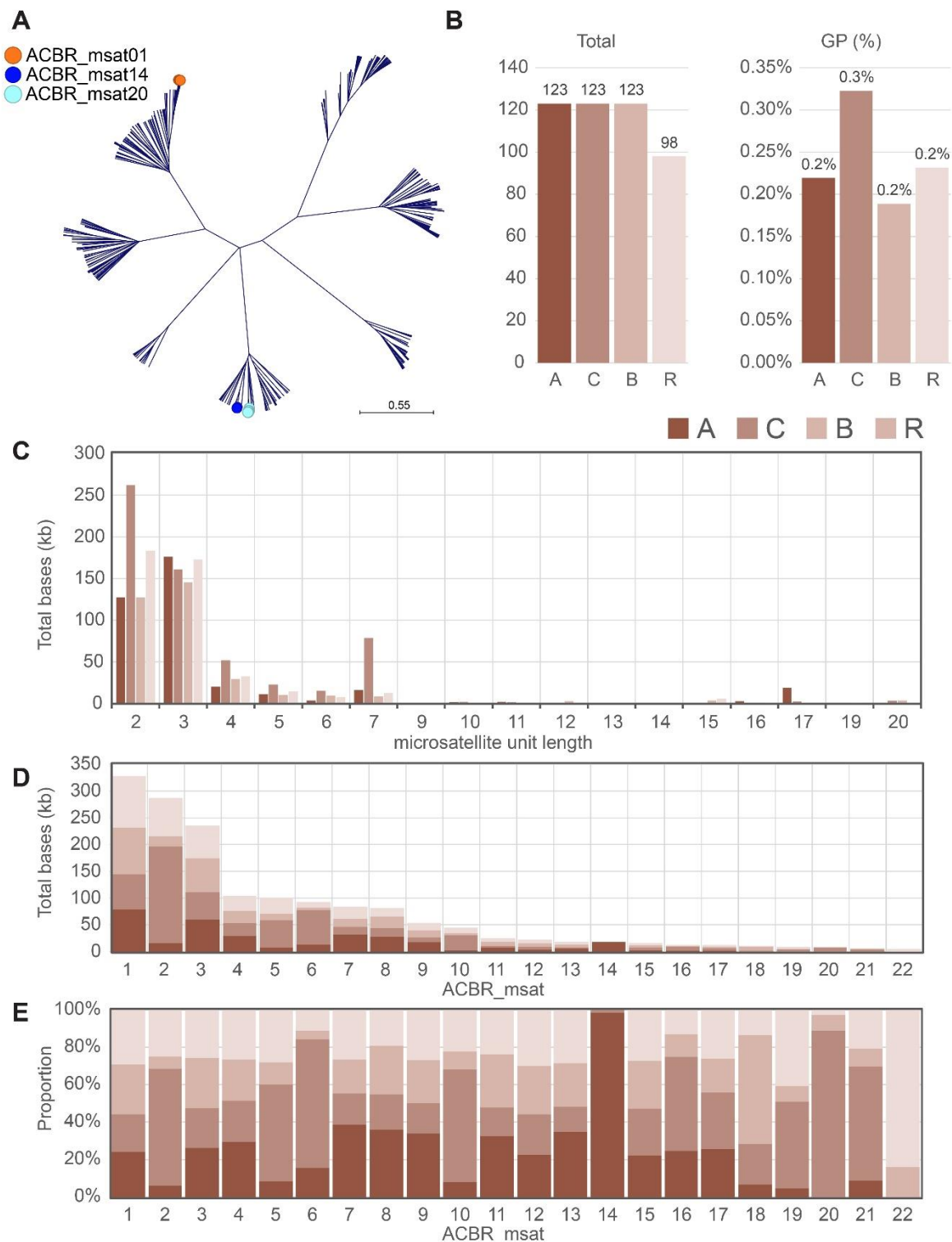


**Figure 1.** Quantification of microsatellites in the A, C, B, and R genomes. **(A)** Clustering of 467 microsatellites that were  $\leq 20$  bp in the A, B, C, and R genomes. The three microsatellites that showed genome-specific distribution are shown in circles. **(B)** Distribution of the 467 microsatellites by genome in terms of total counts and genome proportions (GP). **(C)** Abundance of microsatellites according to monomer length. **(D)** Cumulative base count of the 22 microsatellites that had a cumulative base count of  $\geq 6$  kb. The numbers in the x-axis correspond to the microsatellite names listed in Table 3. **(E)** Cumulative proportion of each microsatellite in the A, C, B, and R genomes. Note the predominant abundance of ACBR\_msat14 and ACBR\_msat20 in the A and C genomes, respectively. ACBR\_msat01 showed relative equal abundance in the four genomes. Bar graph colors in C–E are same as those in B.

**Table 3.** Summary of top 22 microsatellites identified in the A, C, B, and R genomes.

| Name        | Sequence          | Length | Total Bases |         |        |        | Grand Total |
|-------------|-------------------|--------|-------------|---------|--------|--------|-------------|
|             |                   |        | A           | C       | B      | R      |             |
| ACBR_msat01 | AG                | 2      | 80,004      | 65,645  | 87,523 | 95,545 | 328,717     |
| ACBR_msat02 | TA                | 2      | 17,429      | 180,550 | 18,852 | 71,783 | 288,614     |
| ACBR_msat03 | AAG               | 3      | 62,101      | 50,474  | 63,611 | 61,099 | 237,285     |
| ACBR_msat04 | TGA               | 3      | 31,243      | 23,210  | 23,246 | 28,005 | 105,704     |
| ACBR_msat05 | TAA               | 3      | 8541        | 51,851  | 11,968 | 28,179 | 100,539     |
| ACBR_msat06 | TTTAGGG           | 7      | 14,629      | 64,754  | 4438   | 10,471 | 94,292      |
| ACBR_msat07 | TTG               | 3      | 33,032      | 14,323  | 15,292 | 22,713 | 85,360      |
| ACBR_msat08 | TG                | 2      | 29,815      | 15,745  | 21,198 | 16,033 | 82,791      |
| ACBR_msat09 | GAG               | 3      | 18,862      | 8880    | 12,870 | 14,823 | 55,435      |
| ACBR_msat10 | AAAT              | 4      | 3720        | 27,736  | 4390   | 10,228 | 46,074      |
| ACBR_msat11 | ACC               | 3      | 8494        | 4084    | 7375   | 6254   | 26,207      |
| ACBR_msat12 | CTTT              | 4      | 5361        | 5163    | 6096   | 7137   | 23,757      |
| ACBR_msat13 | TGC               | 3      | 6967        | 2710    | 4611   | 5726   | 20,014      |
| ACBR_msat14 | TTTAGGGTTAGGTAGGG | 17     | 18,903      | 297     | 0      | 0      | 19,200      |
| ACBR_msat15 | AAAC              | 4      | 3933        | 4403    | 4519   | 4813   | 17,668      |
| ACBR_msat16 | TTCGG             | 5      | 3505        | 7088    | 1709   | 1843   | 14,145      |
| ACBR_msat17 | ACT               | 3      | 3484        | 4086    | 2441   | 3552   | 13,563      |
| ACBR_msat18 | ATAG              | 4      | 850         | 2701    | 7258   | 1684   | 12,493      |
| ACBR_msat19 | ATTTT             | 5      | 509         | 4749    | 866    | 4191   | 10,315      |
| ACBR_msat20 | TTTCGGG           | 7      | 0           | 8845    | 835    | 270    | 9950        |
| ACBR_msat21 | AATT              | 4      | 722         | 4925    | 792    | 1661   | 8100        |
| ACBR_msat22 | TGAACAGTGTTCGA    | 15     | 0           | 0       | 973    | 5126   | 6099        |

The lengths of the 22 microsatellites ranged from 2 to 17 bp. However, the most abundant microsatellites were di- and trinucleotides. Moreover, 7-bp microsatellites were also abundant, although significantly biased to the C genome (Figure 1C). The 7-bp microsatellites represented the canonical *Arabidopsis*-type plant telomere repeat, ACBR\_msat06, and its variant, ACBR\_msat20 (Table 3). The *Arabidopsis*-type telomeric repeat covered ~65 kb total bases in the C genome, whereas only <15 kb in the other genomes. The ACBR\_msat20, which was also observed predominantly in the C genome, had the central “A” in the *Arabidopsis*-telomeric repeat sequence replaced with a “C”.

Furthermore, microsatellites comprising only T and A were predominantly abundant in the C genome (Table 3). Although this bias was observed in di-, tri-, tetra, and pentanucleotides, it was prominent in the TA dinucleotide microsatellite (ACBR\_msat02), in which the C genome had a total base of ~180 kb, whereas the A and B genomes had only < 20 kb and the R genome was ~71 kb (Table 3). The biased abundance of several microsatellites toward the C genome explains the higher proportion of microsatellites in the C genome than in the other three genomes (Figure 1B).

Similarly, ACBR\_msat14 showed a biased abundance in the A genome (Figure 1E and Table 3). ACBR\_msat14 is a 17-bp higher-order organized *Arabidopsis*-type telomere repeat composed of two units and an insertion of a trinucleotide “AGG” in the second repeat unit, particularly between the second and third T nucleotides (Table 3).

Some microsatellites, such as ACBR\_msat18 and ACBR\_msat22, also showed biased abundance in the B and R genomes, respectively. However, whether these genome-specific biases in microsatellite abundance also reflect their usability as genome-specific cytogenetic markers should be verified by FISH.

### 3.2. FISH Revealed Different Chromosome and Genome Distribution Patterns of the Microsatellites

To visualize the chromosomal distribution of the 22 microsatellites and analyze whether the microsatellites that showed putative genome specificity based on the in-silico analysis could also generate genome-specific FISH signals, we performed the FISH analysis in the four diploid A, C, B, and R genomes using PLOPs developed from the 22 microsatellite sequences (Supplementary Table S1).

Eleven of the 22 microsatellites did not show detectable FISH signals, indicating non-clustering of the microsatellite loci [46], making them undetectable by FISH (Supplementary Figure S3 and Table S1). Other microsatellites showed clustered loci that generated detectable FISH signals in either a few or all chromosomes in each genome. One microsatellite showed signals in the A, C, and B genomes, whereas five showed non-specific signals for all four genomes. Two microsatellites showed signals in both the C and R genomes, and one microsatellite showed specific signals to the A (ACBR\_msat14) and C (ACBR\_msat20) genomes (Figures 2 and 3, Table 3). We did not observe any microsatellite that discriminated the B and R genomes. However, we identified one microsatellite that showed signals to both B and R genomes (ACBR\_msat01) (Supplementary Figure S3, Figures 2 and 3, Supplementary Table S1).

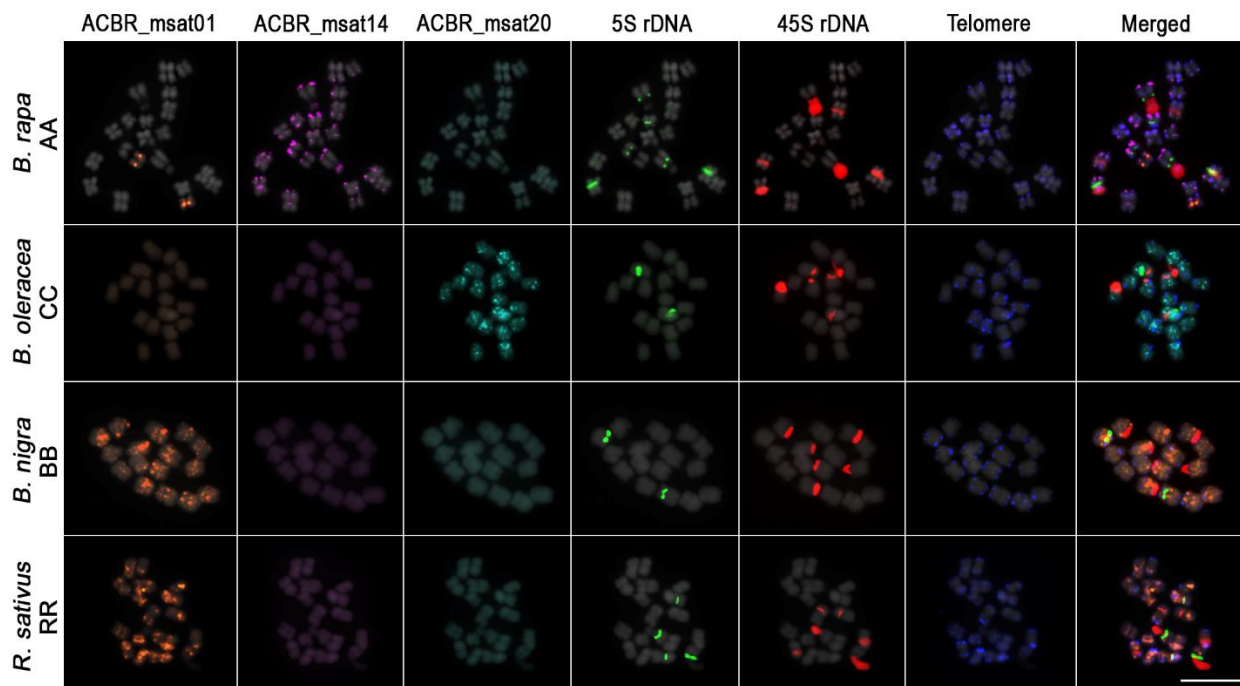


**Figure 2.** FISH analysis of ACBR\_msat01, ACBR\_msat14, and ACBR\_msat20 in the four diploid genomes. ACBR\_msat14, and ACBR\_msat20 were exclusively detected in *B. rapa* and *B. oleracea* genomes, respectively. ACBR\_msat01 was detected in both *B. nigra* and *R. sativus* genomes including one pair of *B. rapa* chromosomes. Scale bar = 10  $\mu$ m.

Genome-specific abundance from the in-silico analysis was partially supported by FISH data. The *Arabidopsis*-type telomeric repeat showed biased intense signals in the C genome, corroborating in silico data (Supplementary Figure S4 and Table S1). In addition, ACBR\_msat14 and ACBR\_msat20 showed A and C genome-specific signals, which also corroborated the in-silico data (Supplementary Figure S3, Figures 2 and 3, Supplementary Table S1). However, ACBR\_msat01 showed signals only in the B and R genomes as well as in one chromosome pair in the A genome. This did not coincide with the in-silico data, where relatively equal abundance in the four genomes was observed (Figures 1E, 2, and 3, Table 3). These data suggest differences in the loci organization of this microsatellite in the four genomes: clustered in the B and R genomes as well as in chromosome 8 in the A genome and non-clustered in the C genome and other chromosomes in the A genome.

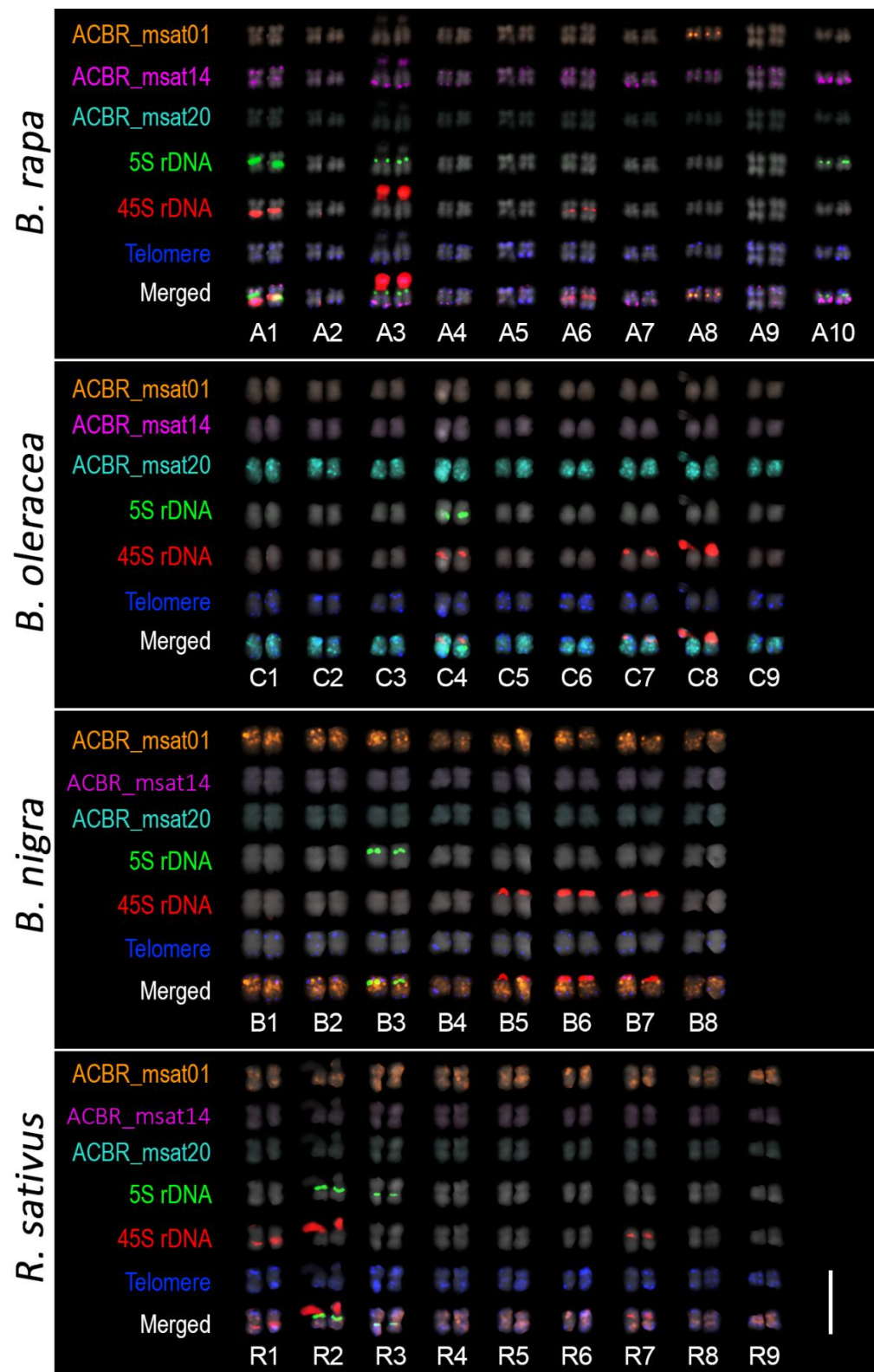


**Figure 3.** Karyogram of *B. rapa*, *B. oleracea*, *B. nigra*, and *R. sativus* chromosomes from Figure 2. The chromosomal distribution of ACBR\_msat01, ACBR\_msat14, ACBR\_msat20, 5S rDNA, 45S rDNA and *Arabidopsis*-type telomere repeats as well as the merged images of the six probes are shown. Note the hybridization of ACBR\_msat01 in chromosome A8. Also note the disperse distribution of ACBR\_msat20 signal in the C genome. Scale bar = 10  $\mu$ m.

In summary, the FISH analysis revealed three microsatellites specific to the diploid species in the U's triangle: ACBR\_msat14 for the A genome, ACBR\_msat20 for the C genome, and ACBR\_msat01 for the B genome (Supplementary Figure S3). Additionally, ACBR\_msat01 could also detect R-genome chromosomes, making it a candidate marker for identifying the R chromosomes in the intergeneric  $\times Brassicoraphanus$  hybrids.

### 3.3. Genome-Specific Microsatellites Discriminated Subgenomes in Allotetraploids

To verify whether the FISH signals of ACBR\_msat01, ACBR\_msat14, and ACBR\_msat20 in the diploid *Brassica* genomes were genome-specific and could distinguish subgenomes in interspecific and intergeneric hybrids, we performed the FISH analysis in allotetraploids within the U's triangle and  $\times Brassicoraphanus$ .

As expected, the 10, 9, and 8 homologous chromosomes of the A, C, and B genomes were clearly distinguished from each other in *B. napus* (AACC), *B. juncea* (AABB), and *B. carinata* (BBCC) using ACBR\_msat14, ACBR\_msat20, and ACBR\_msat01, respectively (Figures 4–6). The *Arabidopsis*-type telomeric repeat also enabled identification of the C-genome chromosomes in *B. napus* and *B. carinata* (Supplementary Figure S4), making this probe sufficient to distinguish the C-genome chromosomes among the allotetraploids in the U's triangle.

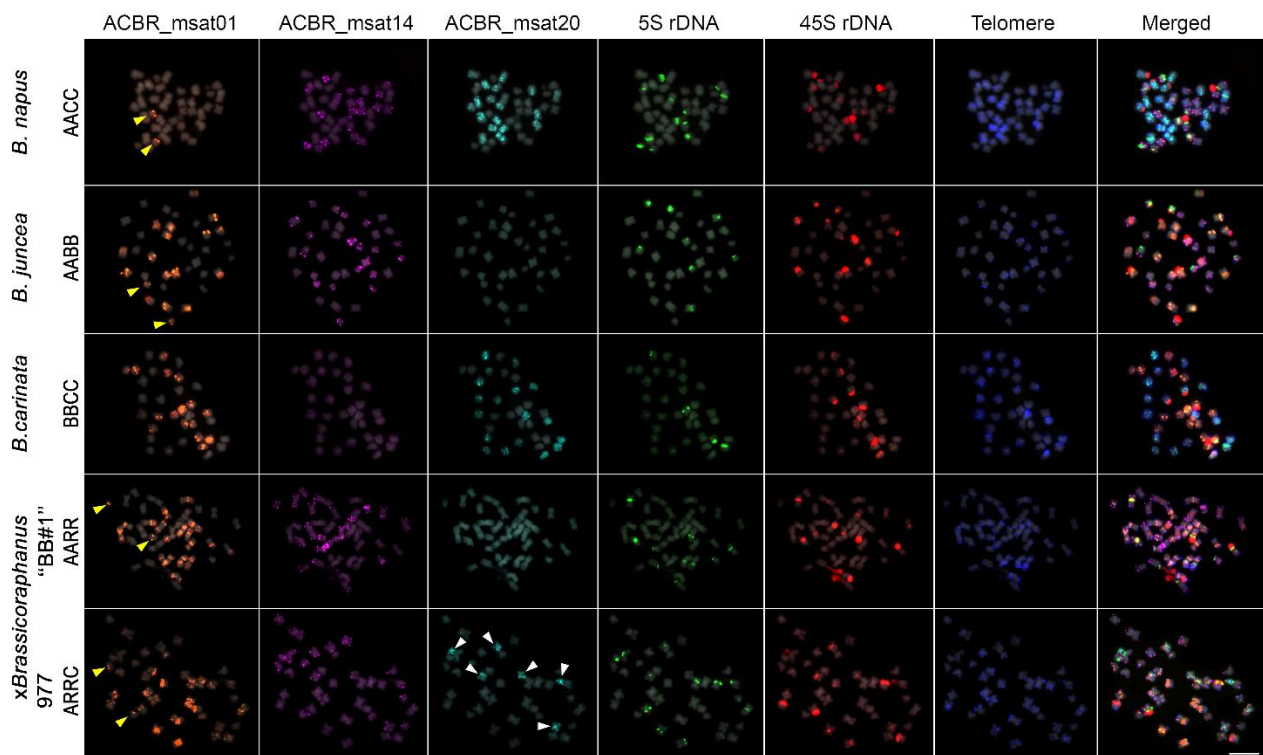


**Figure 4.** FISH analysis of ACBR\_msat01, ACBR\_msat14, and ACBR\_msat20 in *B. napus*, *B. juncea*, *B. carinata*,  $\times Brassicoraphanus$  'BB#1', and  $\times Brassicoraphanus$  977. ACBR\_msat14, and ACBR\_msat20 clearly discriminated the A and C genomes in the allopolyploids, respectively. ACBR\_msat01 was useful in discriminating the B-genome in the interspecific AABB and BBCC allopolyploids, the R genome in the intergeneric AARR genome, and chromosome A8 (yellow arrowheads). Note the six chromosomes with ACBR\_msat20 in  $\times Brassicoraphanus$  977 indicating C-genome chromosome blocks (white arrowheads). Scale bar = 10  $\mu$ m.

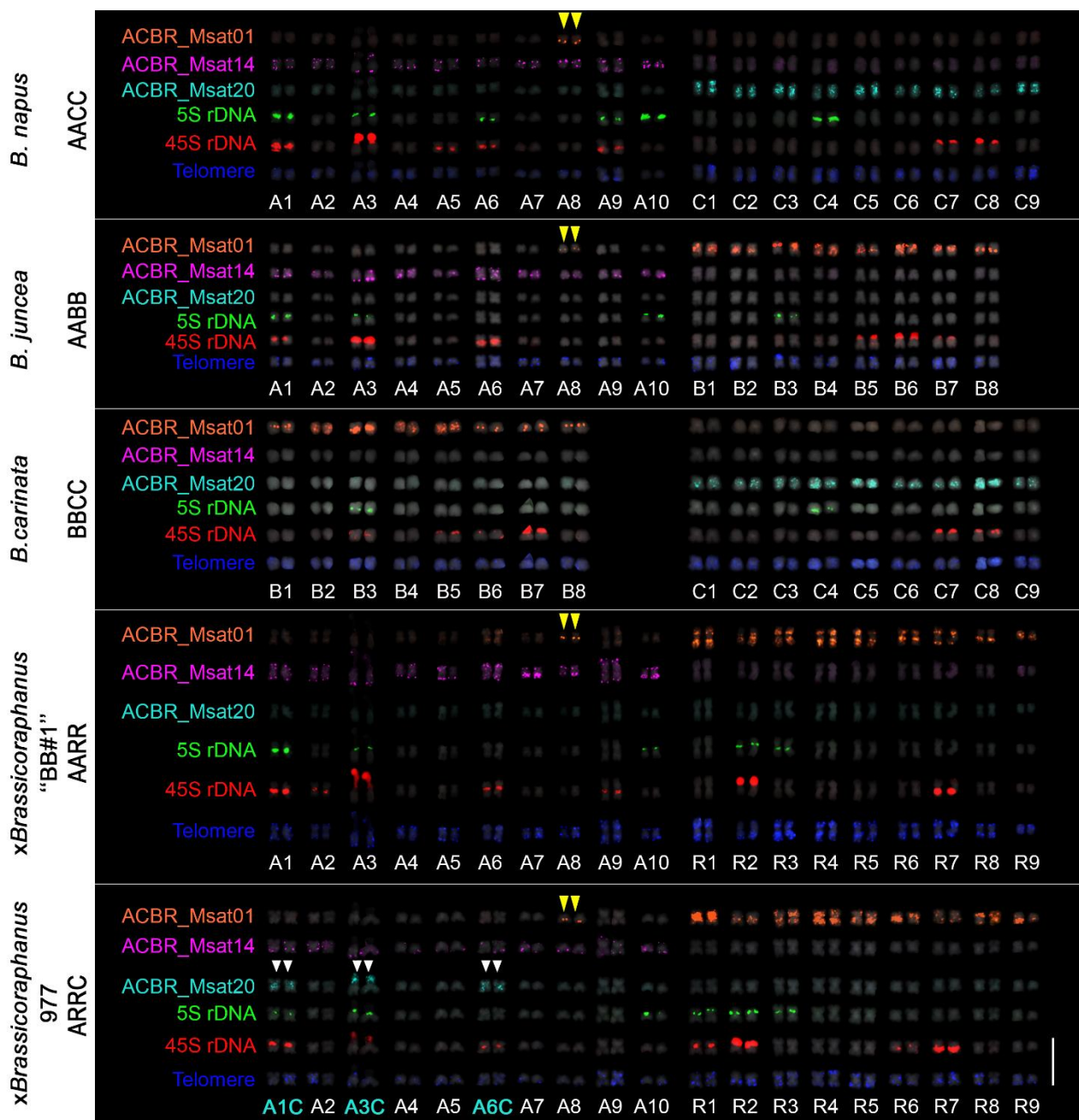


**Figure 5.** Karyogram of natural and synthetic *Brassica* and *Raphanus* allotetraploids. The chromosomal distribution of ACBR\_msat01, ACBR\_msat14, ACBR\_msat20, 5S rDNA, 45S rDNA and *Arabidopsis*-type telomere repeats are shown. ACBR\_msat14 localized at the subterminal with some in the interstitial regions in the A-genome chromosomes (A1–A10). ACBR\_msat20 localized at the interstitial regions of C-genome chromosomes (C1–C9). ACBR\_msat01 localized at the interstitial regions of B-genome chromosomes (B1–B8) and extra signals at the paracentric region of chromosome A8 (yellow arrowheads). A-genome chromosomes with ACBR\_msat20 signals are shown in white arrowheads. Scale bar = 10  $\mu$ m.

Moreover, the A and R genomes were also clearly distinguished in  $\times$ *Brassicoraphanus* “BB#1” using ACBR\_msat14 and ACBR\_msat01, respectively (Figures 4 and 5). However, although the R genome showed intense ACBR\_msat01 signals, A-genome chromosomes also showed ACBR\_msat01 signals in intercalary regions of all chromosomes with varied intensity, although weaker than those in the R genome, except for chromosome 8, which showed a more intense single locus at the proximal region of the long arm (Figure 5).

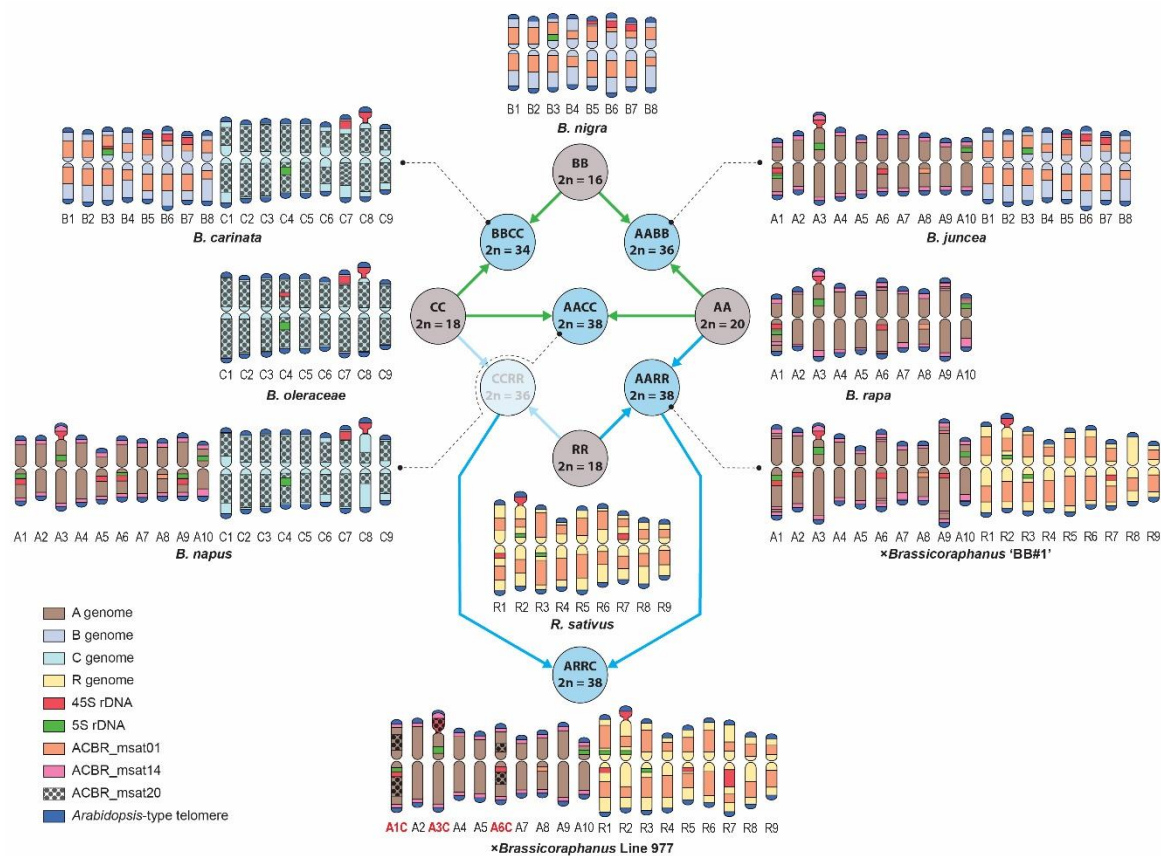


**Figure 6.** Karyotype ideograms and genome relationships between the four diploids and their allotetraploid hybrids. Green arrows show the genome relationships among species within the U's Triangle, and blue arrows for those involving the R genome. The A, C, B, and R genomes are distinguished by chromosome color. The chromosome numbers of  $\times$ Brassicoraphanus 977 with ACBR\_msat20 signals are highlighted red.

In summary, the three microsatellites proved to be efficient FISH probes to distinguish between the A, C, and B subgenomes of the allotetraploid species in the U's triangle and between the A and R genomes in  $\times$ Brassicoraphanus (Figure 6).

### 3.4. FISH Revealed Genome Rearrangement and Chromatin Elimination in $\times$ Brassicoraphanus 977

No cytogenetic analysis has been performed to investigate the chromosomal constitution of the putative tri-genome  $\times$ Brassicoraphanus 977. Therefore, we used the genome-specific microsatellites identified in this study to analyze the genomic composition of this plant. Line 977 was generated from a cross between two  $\times$ Brassicoraphanus allotetraploids, BB#50 (AARR,  $2n = 4x = 38$ ) and "Mooyangchae" (CCRR,  $2n = 4x = 36$ ). Therefore, we expected to see the complete set of the R chromosomes and a mixture of A and C chromosomes.

As expected,  $\times$ Brassicoraphanus 977 had  $2n = 38$  chromosomes, and ACBR\_msat01 identified the complete R-genome chromosomes (Figure 5). ACBR\_msat14 generated signals in the remaining 10 homologous pairs, indicating the A-genome origin of the other chromosomes. ACBR\_msat20 generated FISH signals in three A-genome chromosomes, which we named A1C, A3C, and A6C, indicating introgression of C genome chromosome blocks into these chromosomes (Figures 5 and 6). These data also suggest that the C genome chromatin is preferentially eliminated in  $\times$ Brassicoraphanus 977. The ACBR\_msat20 signals were coincidentally localized in the 45S rDNA-bearing chromosomes and co-localized with the NOR signals. This observation indicates a role for 45S rDNA in the genome reshuffling of the A and C genomes and the homing of the ACBR\_msat20 in the 45S rDNA array in  $\times$ Brassicoraphanus 977.

In summary, the FISH data of the genome-specific microsatellite probes in  $\times$ Brassicoraphanus 977 suggests the possibility that line 977 has an AARR genomic background with introgressed

C-genome chromatin at the 45S rDNA loci, contrary to ARRC that was initially thought. This analysis also showed preferential elimination of the C genome in  $\times Brassicoraphanus$  977.

### 3.5. Ribosomal DNA and Telomeric Repeat Distribution

We used 5S and 45S rDNA probes to identify known chromosomes and the *Arabidopsis*-type telomeric repeats to identify chromosome ends for karyotyping. All four diploid species revealed three 45S rDNA loci, whereas *B. rapa*, *B. nigra*, *B. oleracea*, and *R. sativus* had three, one, one, and two 5S rDNA loci, respectively, similar to those observed in previous studies [5,47–49]. In the allotetraploid species, *B. juncea*, *B. napus*, *B. carinata*,  $\times Brassicoraphanus$  “BB#1”, and 977 had four, six, two, five, and six 5S rDNA loci and six, seven, six, five, and seven 45S rDNA loci. *Arabidopsis*-type telomeric repeat sequences were detected in all chromosomes of *Brassica* and *Raphanus* genome.

## 4. Discussion

### 4.1. Importance of Subgenome Discrimination in Allopolyploids

The ability to discriminate individual subgenomes or chromosomes in allopolyploids is invaluable for studying genome structure, dynamics, and stability [26,50]. This is particularly useful in analyzing the chromosomal composition and genetic stability of synthetic plants from intergeneric crosses, such as  $\times Brassicoraphanus$ , which generate sterile progenies from unstable meiotic chromosome pairing [51].

Although GISH has been the conventional choice to discriminate subgenomes in allopolyploids [20,21], recent innovations, such as bulk oligo-FISH which uses single-copy oligomer probes, can allow easy discrimination of subgenomes and individual chromosomes [52]. However, this method requires high-quality genome assembly to design oligoprobe libraries, making it difficult to analyze species without a whole-genome assembly [52,53]. Moreover, the synthesis of bulk oligo libraries is costly relative to repeat-based pre-labeled oligomer probes (PLOPs) [38]. However, several bioinformatics tools (see Methods, for example) offer ways to analyze repeats and microsatellites from short next-generation sequences, enabling microsatellite analysis in species without genome assembly.

Microsatellites can have genome-specific distribution. Therefore, they can be useful in discriminating subgenomes in allopolyploids, as demonstrated in previous studies [25,26,29,54] and this study. Here, we identified 22 high-abundance microsatellites from the A, C, and B genomes of *Brassica* and the R genome of *R. sativus* using short next-generation sequencing reads. Three microsatellites, namely ACBR\_14, ACBR\_20, and ACBR\_01, could discriminate the A, C, and B *Brassica* genomes and the *R. sativus* R genome, respectively, making them useful cytogenomic markers for natural and synthetic allopolyploids carrying the A, C, B, and R genomes.

Moreover, the FISH procedure using microsatellites is more straightforward and not as laborious and resource-intensive as GISH because PLOPs are used instead of genomic and blocking DNA. In addition, the use of rDNA and telomere repeat PLOPs and the new microsatellites enabled efficient homologous chromosome identification in each subgenome.

### 4.2. Organization of Microsatellite in the Chromosomes Determine FISH Detectability

The abundance of microsatellites in a genome cannot always predict detectability using FISH. Microsatellites are organized either in a clustered or non-clustered manner, making them detectable or undetectable by FISH, respectively [26,46,55–57]. Long microsatellite arrays or short arrays clustered together can allow amplified FISH signals to reach the fluorescence detection threshold [46].

This difference in locus organization was well demonstrated in ACBR\_msat01. Intense ACBR\_msat01 FISH signals were predominantly observed in the B and R genomes, despite being present in comparable abundance in all four genomes based on *in silico* quantification (Figure 1 and Table 3). This pattern suggests a more clustered organization of ACBR\_msat01 in the B and R genomes compared to a predominantly non-clustered organization in the C and A genomes, except for one cluster in chromosome A8.

#### 4.3. Genome-Specific Microsatellites for the A, C, and B Brassica Genomes

Our data corroborated the abundance of a telomeric repeat-like C-genome-specific microsatellite (ACBR\_msat20) previously identified in *B. napus* using conventional molecular techniques [25]. However, although we only identified the consensus TTTCGGG sequence of ACBR\_msat20, a previous study presented an intermittent organization of TTTCGGG, TTTGGGG, and a few imperfect derivative sequences [25], demonstrating that molecular analyses are relevant in defining actual sequences. However, for the FISH and genome discrimination, our results were comparable to previously reported data for discriminating the C-genome chromosomes from the A and B *Brassica* genomes.

In addition to the C genome-specific microsatellite, we identified ACBR\_msat14, which is an A genome-specific microsatellite that efficiently discriminated A from the C and B genomes. Although it is challenging to precisely determine whether ACBR\_msat14 is located in the telomeric or subtelomeric region just by looking at the FISH image, ACBR\_msat14 is possibly localized at the subtelomeric region rather than the telomeres because (i) *Arabidopsis*-type telomeric signals were distinctly observed at chromosomal ends and (ii) subtelomeres are known to host different telomeric sequence variants, similar to the six different variants found in rice subtelomeres [58,59]. Subtelomeres are also prone to accumulation and rapid expansion of several tandem repeats, making subtelomere sites of frequent chromosomal rearrangements [60,61].

Similar to the C and A genomes, we also identified ACBR\_msat01, which discriminated B from the A or C *Brassica* genomes in the U's triangle. However, ACBR\_msat01 failed to discriminate B from the R genome of *R. sativus*. In contrast, ACBR\_msat01 can be an excellent cytogenetic marker between the species in the U's triangle, it would not be useful to distinguish B and R chromosomes in allopolyploids comprising these two genomes. In this case, *B. nigra* and *R. sativus* centromeric satellites may be used to identify the B and R genomes, respectively [62–64]. However, no comparative analysis has been performed in allopolyploids with the B and R genomes that show genome specificity and a lack of cross-hybridization of these centromeric satellites.

#### 4.4. Microsatellite Distribution Supports Phylogenetic Relationships of the Four Diploid Species

The distribution of the three genome-specific microsatellites reflected the phylogenetic relationships of the diploid species. Clustering of the ACBR\_msat01 in the B and R genomes, but not in the A and C genomes, corroborates the observed closer relationship between *B. nigra* and *R. sativus* than *B. nigra* is to the *B. rapa* or *B. oleracea* [37]. Considering the high evolvability of microsatellites [65], the relatively recent divergence of the *B. rapa* and *B. oleracea* genomes from the more primitive *B. nigra* and *R. sativus* [5,37] may have abruptly de-clustered the ACBR\_msat01 loci in the C genome and most of the A genome, except for that chromosome A8. This genome reshuffling may have also concomitantly spurred the differential evolution of telomere-like repeats between the A and C genomes.

#### 4.5. Association of 45S rDNA in Genome Reshuffling

Several studies have implicated the involvement of the 45S rDNA array in plant genome rearrangements [60,66–68]. Similarly, we observed the participation of the 45S rDNA array in the rapid evolution of the ACBR\_msat20 microsatellite in  $\times$ *Brassicoraphanus* 977. While the ACBR\_msat20 microsatellite was dispersed in the C-genome chromosomes of the diploid and allopolyploid species in the U's triangle, it was localized at the 45S rDNA loci in  $\times$ *Brassicoraphanus* 977. This observation further demonstrates the role of 45S rDNA in genome reshuffling. Although we have not characterized the sequence of the 45S rDNA in  $\times$ *Brassicoraphanus* 977, the ACBR\_msat20 microsatellite must have been likely inserted into the 45S rDNA intergenic spacer, as this region is often considered a “logistics hub” of repeats in the genome, hosting different types of repeats into or out of the 45S rDNA intergenic spacer [68–70]. The 45S rDNA may also facilitate the rapid and efficient concerted expansion and contraction of genomic repeats, as observed in *Senna* [68] and the ACBR\_msat20 microsatellite in  $\times$ *Brassicoraphanus* 977.

Although the exact mechanism by which 45S rDNA interacts with the genome and performs genome rearrangements is not yet fully understood, microhomology between sub-repeats in the 45S rDNA intergenic spacer and microsatellites may drive recombination, particularly given that microsatellites are known hotspots for recombination and chromosomal rearrangements [71].

## 5. Conclusions

We performed a comprehensive comparative microsatellite quantification and FISH analysis between the *Brassica* A, C, B, and *R. sativus* R genomes and identified three microsatellites that could discriminate the A, C, and B/R genomes. Along with the 45S and 5S rDNA and the *Arabidopsis*-type telomeric repeats, we efficiently identified the subgenomes and homologous chromosomes of the natural and synthetic allopolyploids between these four genomes. This study presents the first three-genome integrated karyotype of the  $\times$ *Brassicoraphanus* 977. The genome-specific microsatellites studied here could constitute an excellent cytogenomic marker to study several lines of synthetic  $\times$ *Brassicoraphanus*.

Although the ACBR\_msat01 could not distinguish between the B and R genomes, further comparative analysis with longer satellite sequences may generate genome-specific probes, such as the centromeric repeats identified in the B and R genomes [62–64]. However, further FISH validation is needed to determine whether these centromeric repeats cross hybridize with each other, considering the close genetic distance between the B and R genomes.

We have also shown the rapid evolution of the ACBR\_msat20 microsatellite and implied the involvement of 45S rDNA in genome reshuffling. Moreover, further sequence characterization of the complete 45S rDNA sequence, including the intergenic spacer in  $\times$ *Brassicoraphanus* 977, will explain the observed signals of the ACBR\_msat20 in the 45S rDNA array and reveal its actual insertion site. This analysis will also help provide clues on the role and mechanism of 45S rDNA in genome rearrangements.

**Supplementary Materials:** The following information is available at <https://www.mdpi.com/article/10.3390/cells10092358/s1>. Figure S1: Breeding summary of  $\times$ *Brassicoraphanus* 977; Figure S2: Summary of the microsatellite mining and FISH validation pipeline; Figure S3: FISH screening of the 22 candidate microsatellites in the diploid *B. rapa* (AA), *B. oleracea* (CC), *B. nigra* (BB), and *R. sativus* (RR) genomes; Figure S4: Chromosomal distribution of *Arabidopsis*-type telomere repeats (ACBR\_msat06) showing more intense FISH signals in 18 C genome chromosomes (yellow arrowheads) in *B. napus* (AACC) and *B. carinata* (BBCC). Table S1: Summary of PLOPs used for FISH.

**Author Contributions:** Conceptualization, N.E.W. and H.H.K.; investigation, N.B.C.; resources, S.-S.L. and J.H.H.; formal analysis, N.E.W.; writing—original draft preparation, N.B.C. and N.E.W.; writing—review and editing, N.E.W., N.B.C., T.H.N., B.Y.K., and H.H.K.; visualization, N.E.W. and N.B.C.; supervision, N.E.W. and H.H.K.; project administration, H.H.K.; funding acquisition, H.H.K., J.H.H., and S.-S.L. All authors have read and agreed to the published version of the manuscript.

**Funding:** This research was funded by a grant from the Agricultural, Fisheries, and Food Technology Planning Evaluation Institute (Research No. 117045033SB020) and by a National Research Foundation of Korea (NRF) grant funded by the Korean government (MSIT) (No. NRF-2020R1G1A1102594).

**Institutional Review Board Statement:** Not applicable.

**Informed Consent Statement:** Not applicable.

**Data Availability Statement:** All data that support the findings of this study are presented in this article and the Supplementary Materials.

**Acknowledgments:** We thank Remnyl Joyce Pellerin for training N.B.C. on FISH analysis.

**Conflicts of Interest:** The authors declare no conflict of interest.

## References

- Kiefer, M.; Schmickl, R.; German, D.A.; Mandáková, T.; Lysak, M.A.; Al-Shehbaz, I.A.; Franzke, A.; Mummenhoff, K.; Stamatakis, A.; Koch, M.A.J.P.; et al. BrassiBase: Introduction to a novel knowledge database on Brassicaceae evolution. *J. Plant Cell Physiol.* **2014**, *55*, e3. [\[CrossRef\]](#)
- Ebeed, H.T. *Bioinformatics Studies on the Identification of New Players and Candidate Genes to Improve Brassica Response to Abiotic Stress*, In *The Plant Family Brassicaceae: Biology and Physiological Responses to Environmental Stresses*; Hasanuzzaman, E., Ed.; Springer Nature: Singapore, 2020; pp. 483–496.
- Mandrigh, L.; Caputo, E.J.N. Brassicaceae-derived anticancer agents: Towards a green approach to beat cancer. *J. Nutr.* **2020**, *12*, 868. [\[CrossRef\]](#)
- Pérez-Balibrea, S.; Moreno, D.A.; García-Viguera, C. Glucosinolates in broccoli sprouts (*Brassica oleracea* var. *italica*) as conditioned by sulphate supply during germination. *J. Food Sci.* **2010**, *75*, C673–C677.
- Waminal, N.E.; Perumal, S.; Lee, J.; Kim, H.H.; Yang, T.-J. Repeat evolution in *Brassica rapa* (AA), *B. oleracea* (CC), and *B. napus* (AACC) genomes. *Plant Breed. Biotechnol.* **2016**, *4*, 107–122. [\[CrossRef\]](#)
- Liu, S.; Liu, Y.; Yang, X.; Tong, C.; Edwards, D.; Parkin, I.A.; Zhao, M.; Ma, J.; Yu, J.; Huang, S. The *Brassica oleracea* genome reveals the asymmetrical evolution of polyploid genomes. *Nat. Commun.* **2014**, *5*, 3930. [\[CrossRef\]](#) [\[PubMed\]](#)
- Nagaharu, U. Genome analysis in *Brassica* with special reference to the experimental formation of *B. napus* and peculiar mode of fertilization. *J. Jap. Bot.* **1935**, *7*, 389–452.
- Khalid, M.; Ayayda, R.; Gheith, N.; Salah, Z.; Abu-Lafi, S.; Jaber, A.; Al-Rimawi, F.; Al-Mazaideh, G. Assessment of antimicrobial and anticancer activity of radish sprouts extracts. *Jordan J. Biol. Sci.* **2020**, *13*, 567–574.
- Chang, M.J.; Kim, B.; Lee, H.S.; Kim, W.K.; Cho, K.J.T.F.J. Anti-cancer effect of Korean radish (*Raphanus sativus* L.) leaf extract through induction of apoptosis and down-regulate Erb B2 signaling and Akt pathway in human breast MDA-MB-231 cell lines. *FASEB J.* **2010**, *24*, 720.4. [\[CrossRef\]](#)
- Lee, S.-S.; Choi, W.-J.; Woo, J.-G. Development of a new vegetable crop in  $\times$ *Brassicoraphanus* by hybridization of *Brassica campestris* and *Raphanus sativus*. *KHSH* **2002**, *43*, 693–698.
- Prakash, S.; Bhat, S.; Quiros, C.; Kirti, P.; Chopra, V. *Brassica* and its close allies: Cytogenetics and evolution. *Plant Breed. Rev.* **2009**, *31*, 21–187.
- Bang, S.; Tsutsui, K.; Shim, S.; Kaneko, Y. Production and characterization of the novel CMS line of radish (*Raphanus sativus*) carrying *Brassica maurorum* cytoplasm. *Plant Breed.* **2011**, *130*, 410–412. [\[CrossRef\]](#)
- Wang, X.; Zeng, L.; Xu, L.; Chen, W.; Liu, F.; Yang, H.; Chi, P.; Ren, L.; Yan, R.; Lu, G. Clubroot resistance introgression in interspecific hybrids between *Raphanus sativus* and *Brassica napus*. *OCS* **2019**, *4*, 139–151.
- Gong, T.; Ray, Z.T.; Butcher, K.E.; Black, Z.E.; Zhao, X.; Brecht, J.K. A novel graft between Pac Choi (*Brassica rapa* var. *chinensis*) and Daikon Radish (*Raphanus sativus* var. *longipinnatus*). *Agronomy* **2020**, *10*, 1464.
- Zhan, Z.; Nwafor, C.C.; Hou, Z.; Gong, J.; Zhu, B.; Jiang, Y.; Zhou, Y.; Wu, J.; Piao, Z.; Tong, Y.J. Cytological and morphological analysis of hybrids between *Brassicoraphanus*, and *Brassica napus* for introgression of clubroot resistant trait into *Brassica napus* L. *PLoS ONE* **2017**, *12*, e0177470. [\[CrossRef\]](#)
- Lee, S.; Kim, H.; Oh, D.; Woo, J.K. Breeding a fertile intergeneric allotetraploid plant between heading Chinese cabbage and Korean radish. *Korean J. Hortic. Sci. Technol.* **1999**, *17*, 653.
- Lee, S.-S.; Lee, S.-A.; Yang, J.; Kim, J. Developing stable progenies of  $\times$ *Brassicoraphanus*, an intergeneric allopolyploid between *Brassica rapa* and *Raphanus sativus*, through induced mutation using microspore culture. *Theor. Appl. Genet.* **2011**, *122*, 885–891. [\[CrossRef\]](#) [\[PubMed\]](#)
- Lee, S.-S.; Son, C.Y.; Kim, J.; Park, J.E.; Yu, S.H.; Yi, G.; Huh, J.H. Properties of self-sterile but cross-fertile allopolyploids synthesized between *Brassica rapa* and *Raphanus sativus*. *Korean J. Hortic. Sci. Technol.* **2020**, *61*, 163–171. [\[CrossRef\]](#)
- Chen, H.; Wu, J. Characterization of fertile amphidiploid between *Raphanus sativus* and *Brassica alboglabra* and the crossability with *Brassica* species. *Genet. Resour. Crop Evol.* **2008**, *55*, 143–150. [\[CrossRef\]](#)
- Schwarzacher, T.; Leitch, A.; Bennett, M.D.; Heslop-Harrison, J. *In situ* localization of parental genomes in a wide hybrid. *Ann. Bot.* **1989**, *64*, 315–324. [\[CrossRef\]](#)
- Ramzan, F.; Younis, A.; Lim, K.-B. Application of genomic *in situ* hybridization in horticultural science. *Int. J. Genomics* **2017**, *2017*, 7561909. [\[CrossRef\]](#)
- Howell, E.C.; Kearsey, M.J.; Jones, G.H.; King, G.J.; Armstrong, S.J. A and C genome distinction and chromosome identification in *Brassica napus* by sequential fluorescence *in situ* hybridization and genomic *in situ* hybridization. *Genetics* **2008**, *180*, 1849–1857. [\[CrossRef\]](#)
- Snowdon, R.; Köhler, W.; Friedt, W.; Köhler, A. Genomic *in situ* hybridization in *Brassica* amphidiploids and interspecific hybrids. *Theor. Appl. Genet.* **1997**, *95*, 1320–1324. [\[CrossRef\]](#)
- Ohmido, N.; Ueda, K.; Fujii, K. Chromosome instability of allopolyploid resynthesized *Brassica napus*. *Chromosome Sci.* **2015**, *18*, 79–84.
- Dos Santos, K.G.B.; Becker, H.; Ecke, W.; Bellin, U. Molecular characterisation and chromosomal localisation of a telomere-like repetitive DNA sequence highly enriched in the C genome of *Brassica*. *Cytogenet. Genome Res.* **2007**, *119*, 147–153. [\[CrossRef\]](#)
- Cuadrado, A.; Cardoso, M.; Jouve, N. Physical organisation of simple sequence repeats (SSRs) in Triticeae: Structural, functional and evolutionary implications. *Cytogenet. Genome Res.* **2008**, *120*, 210–219. [\[CrossRef\]](#) [\[PubMed\]](#)

27. Peakall, R.; Gilmore, S.; Keys, W.; Morgante, M.; Rafalski, A. Cross-species amplification of soybean (*Glycine max*) simple sequence repeats (SSRs) within the genus and other legume genera: Implications for the transferability of SSRs in plants. *Mol. Biol. Evol.* **1998**, *15*, 1275–1287. [[CrossRef](#)] [[PubMed](#)]
28. Karlin, E.F.; Boles, S.B.; Seppelt, R.D.; Terracciano, S.; Shaw, A.J. The Peat Moss *Sphagnum cuspidatum* in Australia: Microsatellites Provide a Global Perspective. *Syst. Bot.* **2011**, *36*, 22–32. [[CrossRef](#)]
29. Santos, J.; Serra, L.; Solé, E.; Pascual, M. FISH mapping of microsatellite loci from *Drosophila subobscura* and its comparison to related species. *Chromosome Res.* **2010**, *18*, 213–226. [[CrossRef](#)]
30. Zhang, L.; Cai, X.; Wu, J.; Liu, M.; Grob, S.; Cheng, F.; Liang, J.; Cai, C.; Liu, Z.; Liu, B. Improved *Brassica rapa* reference genome by single-molecule sequencing and chromosome conformation capture technologies. *Hortic. Res.* **2018**, *5*, 50. [[CrossRef](#)]
31. Paritosh, K.; Pradhan, A.K.; Pental, D. A highly contiguous genome assembly of *Brassica nigra* (BB) and revised nomenclature for the pseudochromosomes. *BMC Genomics* **2020**, *21*, 887. [[CrossRef](#)] [[PubMed](#)]
32. Parkin, I.A.; Koh, C.; Tang, H.; Robinson, S.J.; Kagale, S.; Clarke, W.E.; Town, C.D.; Nixon, J.; Krishnakumar, V.; Bidwell, S.L. Transcriptome and methylome profiling reveals relics of genome dominance in the mesopolyploid *Brassica oleracea*. *Genome Biol.* **2014**, *15*, R77. [[CrossRef](#)]
33. Shirasawa, K.; Hirakawa, H.; Fukino, N.; Kitashiba, H.; Isobe, S. Genome sequence and analysis of a Japanese radish (*Raphanus sativus*) cultivar named ‘Sakurajima Daikon’ possessing giant root. *DNA Res.* **2020**, *27*, dsaa010. [[CrossRef](#)]
34. Novák, P.; Neumann, P.; Macas, J. Global analysis of repetitive DNA from unassembled sequence reads using RepeatExplorer2. *Nat. Protoc.* **2020**, *15*, 3745–3776. [[CrossRef](#)]
35. Benson, G. Tandem repeats finder: A program to analyze DNA sequences. *Nucleic Acids Res.* **1999**, *27*, 573–580. [[CrossRef](#)]
36. Sobreira, T.J.P.; Durham, A.M.; Gruber, A. TRAP: Automated classification, quantification and annotation of tandemly repeated sequences. *Bioinformatics* **2006**, *22*, 361–362. [[CrossRef](#)] [[PubMed](#)]
37. Kim, C.-K.; Seol, Y.-J.; Perumal, S.; Lee, J.; Waminal, N.E.; Jayakodi, M.; Lee, S.-C.; Jin, S.; Choi, B.-S.; Yu, Y. Re-exploration of U’s Triangle *Brassica* species based on chloroplast genomes and 45S nrDNA sequences. *Sci. Rep.* **2018**, *8*, 7353. [[CrossRef](#)]
38. Waminal, N.E.; Pellerin, R.J.; Kim, N.-S.; Jayakodi, M.; Park, J.Y.; Yang, T.-J.; Kim, H.H. Rapid and efficient FISH using pre-labeled oligomer probes. *Sci. Rep.* **2018**, *8*, 8224. [[CrossRef](#)] [[PubMed](#)]
39. Waminal, N.E.; Kim, H.H. Dual-color FISH karyotype and rDNA distribution analyses on four Cucurbitaceae species. *Hortic. Environ. Biotechnol.* **2012**, *53*, 49–56. [[CrossRef](#)]
40. Vrána, J.; Šimková, H.; Kubaláková, M.; Číhalíková, J.; Doležel, J. Flow cytometric chromosome sorting in plants: The next generation. *Methods* **2012**, *57*, 331–337. [[CrossRef](#)] [[PubMed](#)]
41. Lim, K.B.; Yang, T.J.; Hwang, Y.J.; Kim, J.S.; Park, J.Y.; Kwon, S.J.; Kim, J.; Choi, B.S.; Lim, M.H.; Jin, M.; et al. Characterization of the centromere and peri-centromere retrotransposons in *Brassica rapa* and their distribution in related *Brassica* species. *Plant J.* **2007**, *49*, 173–183. [[CrossRef](#)] [[PubMed](#)]
42. Kulak, S.; Hasterok, R.; Maluszynska, J. Karyotyping of *Brassica* amphidiploids using 5S and 25S rDNA as chromosome markers. *Hereditas* **2002**, *136*, 144–150. [[CrossRef](#)] [[PubMed](#)]
43. Belandres, H.R.; Waminal, N.E.; Hwang, Y.-J.; Park, B.-S.; Lee, S.-S.; Huh, J.H.; Kim, H.H. FISH karyotype and GISH meiotic pairing analyses of a stable intergeneric hybrid  $\times$ *Brassicoraphanus* line BB# 5. *Hortic. Sci. Technol.* **2015**, *33*, 83–92.
44. Mehrotra, S.; Goyal, V. Repetitive sequences in plant nuclear DNA: Types, distribution, evolution and function. *GPB* **2014**, *12*, 164–171. [[CrossRef](#)] [[PubMed](#)]
45. Vieira, M.L.C.; Santini, L.; Diniz, A.L.; de Freitas Munhoz, C. Microsatellite markers: What they mean and why they are so useful. *Genet. Mol. Biol.* **2016**, *39*, 312–328. [[CrossRef](#)] [[PubMed](#)]
46. Ruiz-Ruano, F.J.; López-León, M.D.; Cabrero, J.; Camacho, J.P.M. High-throughput analysis of the satellite illuminates satellite DNA evolution. *Sci. Rep.* **2016**, *6*, 28333. [[CrossRef](#)] [[PubMed](#)]
47. Hwang, Y.-J.; Yu, H.-J.; Mun, J.-H.; Bok, K.; Park, B.-S.; Lim, K.-B. Centromere repeat DNA originated from *Brassica rapa* is detected in the centromere region of *Raphanus sativus* chromosomes. *Hortic. Sci. Technol.* **2012**, *30*, 751–756. [[CrossRef](#)]
48. Perumal, S.; Waminal, N.E.; Lee, J.; Lee, J.; Choi, B.-S.; Kim, H.H.; Grandbastien, M.-A.; Yang, T.-J. Elucidating the major hidden genomic components of the A, C, and AC genomes and their influence on *Brassica* evolution. *Sci. Rep.* **2017**, *7*, 17986. [[CrossRef](#)]
49. Xiong, Z.; Pires, J.C. Karyotype and identification of all homoeologous chromosomes of allopolyploid *Brassica napus* and its diploid progenitors. *Genetics* **2011**, *187*, 37–49. [[CrossRef](#)]
50. Chester, M.; Gallagher, J.P.; Symonds, V.V.; da Silva, A.V.C.; Mavrodiev, E.V.; Leitch, A.R.; Soltis, P.S.; Soltis, D.E. Extensive chromosomal variation in a recently formed natural allopolyploid species, *Tragopogon miscellus* (Asteraceae). *PNAS* **2012**, *109*, 1176–1181. [[CrossRef](#)]
51. Belandres, H.R.; Zhou, H.C.; Waminal, N.E.; Lee, S.-S.; Huh, J.H.; Kim, H.H. Cytogenetic analyses revealed different genome rearrangement footprints in four  $\times$ *Brassicoraphanus* lines with different fertility rates. *Plant Breed. Biotechnol.* **2019**, *7*, 95–105. [[CrossRef](#)]
52. Han, Y.; Zhang, T.; Thammapichai, P.; Weng, Y.; Jiang, J. Chromosome-specific painting in *Cucumis* species using bulked oligonucleotides. *Genetics* **2015**, *200*, 771–779. [[CrossRef](#)]
53. Jiang, J. Fluorescence *in situ* hybridization in plants: Recent developments and future applications. *Chromosome Res.* **2019**, *27*, 153–165. [[CrossRef](#)]

54. Cuadrado, A.; Schwarzacher, T.; Jouve, N. Identification of different chromatin classes in wheat using *in situ* hybridization with simple sequence repeat oligonucleotides. *Theor. Appl. Genet.* **2000**, *101*, 711–717. [[CrossRef](#)]
55. Zattera, M.L.; Gazolla, C.B.; de Araújo Soares, A.; Gazoni, T.; Pollet, N.; Recco-Pimentel, S.M.; Bruschi, D.P. Evolutionary dynamics of the repetitive DNA in the karyotypes of *Pipa carvalhoi* and *Xenopus tropicalis* (Anura, Pipidae). *Front. Genet.* **2020**, *11*, 637. [[CrossRef](#)] [[PubMed](#)]
56. Utsunomia, R.; Melo, S.; Scacchetti, P.C.; Oliveira, C.; de Andrade Machado, M.; Pieczarka, J.C.; Nagamachi, C.Y.; Foresti, F. Particular chromosomal distribution of microsatellites in five species of the genus *Gymnotus* (Teleostei, Gymnotiformes). *Zebrafish* **2018**, *15*, 398–403. [[CrossRef](#)]
57. Megyeri, M.; Mikó, P.; Farkas, A.; Molnár-Láng, M.; Molnár, I. Cytomolecular discrimination of the A chromosomes of *Triticum monococcum* and the A chromosomes of *Triticum aestivum* using microsatellite DNA repeats. *J. Appl. Genet.* **2017**, *58*, 67–70. [[CrossRef](#)]
58. Mizuno, H.; Wu, J.; Matsumoto, T. Characterization of chromosomal ends on the basis of chromosome-specific telomere variants and subtelomeric repeats in rice (*Oryza sativa* L.). In *Subtelomeres*; Springer: Berlin/Heidelberg, Germany, 2014; pp. 187–194.
59. Mizuno, H.; Matsumoto, T.; Wu, J. Composition and structure of rice centromeres and telomeres. In *Rice Genomics, Genetics and Breeding*; Springer: Berlin/Heidelberg, Germany, 2018; pp. 37–52.
60. Waminal, N.E.; Pellerin, R.J.; Kang, S.-H.; Kim, H.H. Chromosomal mapping of tandem repeats revealed massive chromosomal rearrangements and insights into *Senna tora* dysploidy. *Front. Plant Sci.* **2021**, *12*, 154. [[CrossRef](#)]
61. Vershinin, A.V.; Evtushenko, E.V. What is the Specificity of Plant Subtelomeres? In *Subtelomeres*; Louis, E.J., Becker, M.M., Eds.; Springer: Berlin/Heidelberg, Germany, 2014; pp. 195–209.
62. Schelfhout, C.; Snowdon, R.; Cowling, W.; Wroth, J.M.; Genetics, A. A PCR based B-genome-specific marker in *Brassica* species. *Theor. Appl. Genet.* **2004**, *109*, 917–921. [[CrossRef](#)] [[PubMed](#)]
63. Schelfhout, C.; Snowdon, R.; Cowling, W.; Wroth, J.M. Tracing B-genome chromatin in *Brassica napus* × *B. juncea* interspecific progeny. *Genome* **2006**, *49*, 1490–1497. [[CrossRef](#)]
64. He, Q.; Cai, Z.; Hu, T.; Liu, H.; Bao, C.; Mao, W.; Jin, W. Repetitive sequence analysis and karyotyping reveals centromere-associated DNA sequences in radish (*Raphanus sativus* L.). *BMC Plant Biol.* **2015**, *15*, 105. [[CrossRef](#)] [[PubMed](#)]
65. Flynn, J.M.; Long, M.; Wing, R.A.; Clark, A.G. Evolutionary dynamics of abundant 7-bp satellites in the genome of *Drosophila virilis*. *Mol. Biol.* **2020**, *37*, 1362–1375. [[CrossRef](#)]
66. Havlová, K.; Dvořáčková, M.; Peiro, R.; Abia, D.; Mozgová, I.; Vansáčová, L.; Gutierrez, C.; Fajkus, J. Variation of 45S rDNA intergenic spacers in *Arabidopsis thaliana*. *Plant Mol. Biol.* **2016**, *92*, 457–471. [[CrossRef](#)]
67. Garcia, S.; Kovařík, A.J.H. Dancing together and separate again: Gymnosperms exhibit frequent changes of fundamental 5S and 35S rRNA gene (rDNA) organisation. *Heredity* **2013**, *111*, 23–33. [[CrossRef](#)] [[PubMed](#)]
68. Ta, T.D.; Waminal, N.E.; Nguyen, T.H.; Pellerin, R.J.; Kim, H.H. Comparative FISH analysis of *Senna tora* tandem repeats revealed insights into the chromosome dynamics in *Senna*. *Genes Genom.* **2021**, *43*, 237–249. [[CrossRef](#)] [[PubMed](#)]
69. Almeida, C.; Fonsêca, A.; dos Santos, K.G.B.; Mosiolek, M.; Pedrosa-Harand, A.J.G. Contrasting evolution of a satellite DNA and its ancestral IGS rDNA in *Phaseolus* (Fabaceae). *Genome* **2012**, *55*, 683–689. [[CrossRef](#)] [[PubMed](#)]
70. Falquet, J.; Creusot, F.; Dron, M. Molecular analysis of *Phaseolus vulgaris* rDNA unit and characterization of a satellite DNA homologous to IGS subrepeats. *Plant Physiol.* **1997**, *35*, 611–622.
71. Dos Santos, J.M.; Diniz, D.; Rodrigues, T.A.S.; Cioffi, M.D.B.; Waldschmidt, A.M. Heterochromatin distribution and chromosomal mapping of microsatellite repeats in the genome of Frieseomelitta stingless bees (Hymenoptera: Apidae: Meliponini). *Fla. Entomol.* **2018**, *101*, 33–39. [[CrossRef](#)]